Development of low pressure cold sprayed copper coatings on carbon fiber reinforced polymer (CFRP)

V. Gillet, E. Aubignat, S. Costil, Bruno Courant, C. Langlade, Pascal Casari, W. Knapp, M.P. Planche

Development of Low Pressure Cold Sprayed Copper Coatings on Carbon Fiber Reinforced Polymer (CFRP)

V. Gillet[1,3*], E. Aubignat[2], S. Costil[2], B. Courant[3], C. Langlade[2], P. Casari[3], W. Knapp[4], M.P. Planche [2]

[1] Coopération Laser Franco-Allemande (CLFA), Paris, France
[2] ICB-LERMPS UMR6303, Univ. Bourgogne Franche-Comté, UTBM, F-90100 Belfort cedex, France
[3] Institut de Recherche en Génie Civil et Mécanique (UMR CNRS 6183), Université de Nantes, Saint-Nazaire, France
[4] Fraunhofer-Institut für Lasertechnik (ILT), Aachen, Germany

*E-mail: vincent.gillet1@univ-nantes.fr
Tel: +33 (0)2 72 64 87 52

Abstract

A new method which allows the development of Low Pressure Cold Sprayed copper coatings on PEEK (Poly-Ether-Ether-Ketone) based composites reinforced by carbon fibers is investigated. Due to the solid state and high velocities of impacting particles, cold spraying involves a high erosion on composite materials, leading to an absence of coatings and sometimes damaged carbon fibers. As a result, few dozen micrometers of pure PEEK matrix have been added on the surface of the composite to act as an interfacial layer between composite and coating. Optimization of the LPCS parameters has been carried out, using a careful choice of powder size distribution in order to avoid substrate damage, erosion and coating delamination.

Dense copper coatings exceeding 100 micrometers thick have been obtained. SEM observations have been carried out to evaluate the microstructure of coatings, and the minimal required matrix thickness regarding the size distribution of the powder.

1 Introduction

Carbon fiber-reinforced polymers (CFRP) are appealing materials due to their unique properties, such as their combination of low density and high mechanical performances [1]. PEEK (Poly-Ether-Ether-Ketone) is a semicrystalline thermoplastic. Its excellent mechanical and chemical resistance properties, associated with high long-term service temperature (220 °C) and fusion temperature (343 °C) makes it widely used in automotive industry, which uses 35% of the PEEK produced worldwide [2]. PEEK is used in pump mechanisms to replace steel and aluminum parts (propeller blades, bearings …). This polymer is also biocompatible and therefore has many medical applications among which implants and prosthesis [3], [4].

Concerning aeronautical and aerospace fields, PEEK is mainly employed as a matrix for carbon fiber reinforced composites [5]. Those composite materials can replace metallic materials in many applications, such as aircraft structures. The main limitations for such application is their electrical resistance. The aircraft structures need to be electrically conductive to avoid the damage from lightning strikes and thunderstorm electric field attacks [6]. Today, different methods are developed to add conductive paths on the surface of structural composite parts. The most commonly used are woven metal fiber or perforated mesh (namely bronze or copper) reinforced composites during the composite fabrication [7]–[9].

Thermal spraying could be an interesting alternative to replace those expensive metallic meshes and allow a better adaptability in used materials, geometry and thickness for the desired conductive layer. Plasma and Arc spraying have already been studied as potential solutions [10], [11] with few successful attempts [12], [13], but such high temperature processes tend to deteriorate the polymer matrix due to molten droplets, instead of building a coating. Cold Spraying offers different benefits such as cost efficiency, portability, ease of use, with a reduced thermal input on substrates compared to other thermal spray processes and produce oxide free coatings. But Cold Sprayed coating on organic materials are difficult to obtain due to the substrate erosion sensitivity [14] and other specific characteristics of such materials, such as a temperature-dependent thermal [15] and mechanical properties [16].

Glass transition temperature (T_g) is the temperature where a thermoplastic material switches between a relatively brittle and hard state to a softer and rubbery state. Below T_g all polymer molecules are confined with a very limited freedom of movement and a small free volume. Above T_g molecules have more freedom of movement and can shift or slide away from each other. T_g of the PEEK is estimated between 146 °C and 153 °C depending on the experimental conditions [15], [16]. Studies have shown that on a thermoplastic polymer the heat input induced by the nozzle is high enough to reach T_g and therefore soften the substrates. Therefore cold sprayed metal particles penetrate deeply inside the polymer without deformation, polymer flooding and sometimes including particles few dozen micrometers beneath substrate surface, creating a mixed metal/polymer interface on which a coating can sometimes be obtained under proper conditions [14], [17], [18].

The first aluminum coatings were obtained on CFRPs in 2011 [19]. Thus, a two step spray operation has been investigated by using plasma-spray process to obtain a thin aluminum layer followed by another layer via cold spraying. In order to improve the electrical conductivity of organic materials, copper coatings have been experimented on CFRPs in 2014 using cold spraying. [20]. Metallic coatings have been successfully sprayed using a tin/copper composite powder [21]. However tin is prohibited for aeronautical applications due to its low transition temperature at 13.2 °C [22]. In 2016, G. Archambault and al. proposed an innovative solution. Instead of direct spraying on the composite, the coating was elaborated on the Invar mold used for lay-up molding process [23]. During the molding process, a direct contact between the molten matrix and the copper coating occurred via mechanical anchoring due to coating roughness. Since it has a low adherence, the coating is transferred onto the composite after unmolding. In 2018, H. Che and al. demonstrated the existence of a deposition window for copper on PEEK using both Low Pressure and High Pressure Cold Spray [24].

Spraying copper directly on PEEK-based CFRPs substrates is investigated. The present work demonstrates that a polymer layer protecting the carbon fibers on top of the substrate is needed. A controlled coating construction strategy was applied to consider the powder granulometry influence.

2   Experimental procedure

2.1   Materials

In this study, a composite material made of carbon fibers and PEEK resin produced by Pipreg Porcher Industries (Badinières, France) was used [25]. This Pipreg composite is an aeronautical qualified laminate (Ref. L03106-57100602) composed of 6 stacks of carbon fibers with a sequence of [(0,90)/(+45,-45)/(0,90)]s, for a total thickness of 1.86 mm. Varying the external PEEK layer thickness, three different composites have been carried out using a PEEK film (Lite TK) produced by Lipp-Terler GmbH (Gaflenz, Austria) [26], with a thickness of 50 µm and 0.5% carbon as filler as presented in Figure 1.

Coatings were produced by spraying spherical Cu - 0.1% Ag powders elaborated by gas atomization at UTBM. The original powder was sieved into three batches with different size distributions named as Fine (F), Medium (M) and Large (L) as presented in Table 1 and Figure 2. The three powders (Figure 3) cover classical size range for Cold Spray particles, with a median diameter of 10.1 µm (F), 23.2 µm (M) and 37.9 µm (L).

2.2   Coating production

Copper coatings are obtained by Low Pressure Cold Spraying (LPCS) using the commercially available Dycomet 423 system (Akkrum, Netherland s) equipped with a 6mm-diameter K6 nozzle mounted on a 6-axis ABB robot (XYZ). To elaborate a homogeneous layer on top, a regular movement was programed for the robot perpendicular to the surface including cooling period between each transversal pass on the substrate. To lower the thermal input on substrates, a large step has been fixed between each pass (3 mm) and a second program is superposed with 1.5 mm offset from the original position to obtain a homogeneous coating regarding thickness (Figure 4). The spray parameters are listed in Table 2, with a predefined temperature level set at 3 on the system. Temperature level is a result of previous trial, this level allowing to imping easily some copper particles on the substrate, without damaging it. Gas temperature has been measured by a thermocouple placed at the nozzle outlet. Gas pressure was fixed at usual working value for this Dycomet system.

Gas flow was fixed during all experiments. Due to their different granulometries, powder feed rates presented some differences between the three powders: 15.7 g/min for the Fine powder, 20.6 g/min for the Medium and 18.0 g/min for the Large one.

Depending on samples, one or several layers have been sprayed to increase the coating thickness. According to the powder granulometry as well as the composites including different PEEK layer thicknesses, several strategies have then been investigated. A code X/X/X was set to label the samples by the combination of powders used to build the coating. For example, a sample labeled as F/M/L shows that a first layer was deposited using Fine powder followed by a second layer using Medium powder and finally a third layer using the Large one. Samples with only two layers have a two letter code.

2.3   Characterization methods

2.3.1   Microscopy analysis

Microscopic observations were carried out using optical and scanning electron microscope, in order to check the quality and measure the thickness of sprayed coatings.

Scanning electron microscope is a Zeiss EVO 40 with a CZ BSD detector (BackScattered electron Detector). Observations were made under Extended Pressure conditions, in order to use a nitrogen flow inside the SEM chamber to avoid electrical charge accumulation on the PEEK parts (under the electron beam), which can induce surface defects on SEM pictures.

Optical microscope is a Nikon Inverted Microscope Epiphot-TME, coupled with the Perfect Image software for picture acquisition.

Samples were embedded in an epoxy mounting resin and polished to obtain a suitable surface for microscopic observations. Grinding has been made using successively P260, P500, P800, P1200 and P4000 SiC grinding papers, followed by a polishing sequence using 3µm and 1µm diamond based solutions. Some of them were in a second step chemically etched (5g iron (III) chloride, 2 mL hydrochloric acid and 96 mL ethanol) to reveal inter-particle joints in the coating and study the particle size distribution.

Due to the roughness of coatings, a statistical measurement has to be performed to quantify their thickness. Thickness was obtained by taking two cross-section pictures, then making

seven equally spaced thickness measurements on both pictures. Thickness is then considered as the average of 14 measurements.

Coating porosity characterization was carried out by taking five SEM pictures of each sample (Grand. 800X) and applying a thresholding technique on pictures using GIMP software.

2.3.2 Deposition Efficiency

Characterization of the Deposition efficiency (DE) is required for industrial applications. DE is defined as the ratio (1) of the weight of the adhered particles (m_{coat}, g) to the total weight of the sprayed particles (m_{th}, g).

$$DE = \frac{m_{coat}}{m_{th}} * 100 \qquad (1)$$

Theoretical mass is calculated by using relationship (2).

$$m_{th} = \frac{\rho_v * S * W}{V * 60} \qquad (2)$$

Where:

- ρ_v is the measured mass flow rate of powder (g/min)
- S is the number of spraying scans of the nozzle on the substrate (8 for one layer)
- W is the width of the substrate (mm)
- V is the transversal speed of the robot (100 mm/s)

Masses are measured using a Sartorius scale model CP64 (precision 0.1mg). Mass flow rate is determined by unplugging the pipe conveying the powder to the spray gun, activating the powder feeder for one minute and measuring powder conveyed mass.

Deposition efficiency (DE) was systematically calculated after each deposited layer. The sample is then removed from the sample holder, its mass is measured and it is replaced on sample holder to spray the next layer. Multi-layer samples are obtained in the same experiment but with a delay time between each layer to measure the mass. It allowed to track the DE evolution during building up the coating and also provided an improved statistical approach to study the first deposited layers DE.

2.3.3 Electrical resistivity

In order to evaluate the electrical conductivity of coatings, electrical resistivity measurements were performed by using a four-point-probe technique at room temperature [27]. Measurement cell is a certified multiheight probe produced by Jandel (Linslade, the UK),

composed of four equally spaced (1 mm) tungsten carbide tips inducing a current into the sample. The electrical resistance of the sample is measured. Resistivity (R_0) is calculated via the relationship (3) where 4.532 is a correction factor regarding the shape of the cell, t the thickness of the tested coating and R_m the measured electrical resistance [28].

$$R_0 = 4.532 * R_m * t \qquad (3)$$

The electrical resistance R_m is measured at 16 different points of each tested sample and then averaged to determine the resistivity R_0.

2.3.4 In-flight Particles Velocity Measurements

In-flight particle velocity was necessary to estimate the induced kinetic energy of impacting particles on substrates. Particle velocity measurements were performed using DPV-2000 dual-slit velocimeter (Tecnar Automation Ltd., St. Bruno, Canada). This system is based on a 785 nm laser illuminating particles in the spray plume. Those particles pass in front of a two-slit photomask equipped with an optical sensor head, and generate a two-peak signal. Particle velocity can then be calculated as the flight time divided by the distance between the gaps.

3 Results and Discussions

A careful optimization of the spray parameters is the most common solution to obtain uniform and dense coatings with usual mechanical properties. In this study the spray parameters were fixed and only the influence of powder granulometry was characterized to obtain the densest and most electrically conductive coatings combined with an acceptable DE.

3.1 Spray Strategy Development for Copper Coatings on organic composite

The industrial Pipreg composite exhibits a quite inhomogeneous surface due to its woven laminate structure. The polymer matrix and carbon fibers are present, with some areas where carbon fibers are really close to the surface and some with apparent organic matrix. During the spray process, an inhomogeneous copper coating is obtained with a remarkable pattern. Areas where carbon fibers lay flush with the surface were eroded, while areas with some organic matrix on the surface were impinged with copper particles (Figure 5). An inhomogeneous coating is obtained and the addition of a second copper layer has led to an extended erosion of the substrate. Considering the different materials included inside the composite, various material behaviors may occur. The high hardness combined with the poor deformation capacity of carbon fibers can justify the erosion of CFRPs [18], [19]. Inversely,

the ductility of organic matrix can allow particle impingement and coating formation when convenient spraying conditions are found.

Regarding these first results, spray tests have been implemented on samples including thicker organic layer on the composite surface. The objective of PEEK film addition is to cover carbon fibers, protect them from impacting copper particles and allow particles impingement on the whole sample surface.

To separate the influence of powder granulometry from the influence of PEEK layer thickness, spray strategies on Single PEEK layer samples (film thickness 57 µm) were carried out first. Due to the low thickness of the PEEK layer on top, excessive erosion of this layer while spraying must be avoided in order to keep the underlying carbon fibers protected. The optimization strategy involved the addition of a second PEEK layer (labeled as Double PEEK samples, 105 µm PEEK film). In this first part of the study only results obtained on Single PEEK samples are presented.

A continuous coating was produced as illustrated in Figure 6a by spraying four layers of Fine powder. A coating thickness of 300 µm was obtained with usual morphological aspects of Cold Spray coatings such as surface rugosity and low porosity. The addition of the 57 µm PEEK layer was enough to produce a coating on the total sample surface. The deposition of a copper coating on modified composites was then demonstrated.

However the obtained coating presents a visible porosity and the interface substrate/coating is uneven, with many defects (Figure 6b). Porosity distribution through coating thickness was calculated by dividing the coating in three equal layers and calculating the porosity in each one. A value of $2.64 \pm 0.62\%$ was obtained at the layer close to the interface with PEEK film, confirming the presence of numerous defects in this layer. Previous studies pointed out that High Pressure Cold Spraying can soften polymer material, leading to particle penetration and squeezing out some substrate material between impinged metallic particles [18], [29]. Zooming in the coating/substrate interface (Figure 6b) the same mechanism was observed for Low Pressure Cold Sprayed coating. Some copper particles were entirely embedded inside the PEEK film, creating a polymer/metal interphase. The substrate surface presents severe deformations, and some squeezed PEEK is spotted around particles. Those behaviors seem

responsible to interfacial defects. Due to the viscosity of the polymer, filling the gap between impacted particles become complex.

Porosity dropped to 0.36 ± 0.04% in the middle of the coating and then increased again to 0.74 ± 0.23% on top layer. This evolution is linked to the hammering or tampering effect, a characteristic of Cold Spray process where incoming particles compact the underlying layers [30]. However, this hammering effect was not efficient enough to compact the interfacial porosities.

Hammering effect is directly linked to the kinetic energy of impacting particles. The influence of the granulometry was investigated by spraying Fine, Medium and Large powders. Table 3 presents surface picture, DE and cross sections for one layer coating deposition attempts using F, M and L powders.

Using Fine powder for the first layer led to a homogeneous copper coating, with around 120 µm thickness and a DE of 28.2 ± 5.5%. The use of Medium and Large powder led to isolated particles or small aggregates impinged at the surface of the PEEK film. The measured DEs were significantly lower, with a value of 8.2 ± 1.2% for M and 5.2 ± 1.2% for L.

Such observations suggest that Medium/Large particles induce too much energy to the substrate during impact which can degrade the coating properties [31]–[33], as confirmed by multiple craters on substrate surface. In order to estimate particles kinetic energy DPV measurements were needed to evaluate the particles velocities regarding their diameter. Characterization of Fine powder was impossible due to the technical limitations of the available equipment, the particle diameter was too small to be detected.

The evolution of in-flight particle velocity regarding their diameter is presented in Figure 7 for Medium and Large powders. Even though the measurements were dispersed, a linear evolution can be approximated as linear and it was observed that mean particle velocity for both Medium and Large powders is close to 400 m/s. Based on the mass transfer phenomena across the shock wave that persist at the nozzle, it was assumed that Fine powder velocity distribution is similar. Kinetic energy of d_{50} particles has therefore been evaluated for each powder (Table 4). A factor of 10 on kinetic energy can be noticed between F ($3.9.10^{-7}$ kg.m².s^{-2}) and M ($4.7.10^{-6}$ kg.m².s^{-2}), which increased to almost 100 between F and L ($2.0.10^{-5}$ kg.m².s^{-2}). These results are related to the deposition behavior of Fine and the erosion behavior of Medium/Large powders.

3.2 Coating thickness enhancement

The objective of this study was to evaluate the feasibility of building thick (100 µm minimum) and dense copper coating on CFRP. In order to increase the thickness and optimize the density, different powders were used to build a coating layer by layer, using F powder to enhance the thickness and M/L powders to compact previously deposited layers.

3.2.1 Addition of a Second Copper Layer

Every possible powder combination was studied, and sample overviews are shown in Figure 8. Three different behaviors can be spotted by visual inspection: building, eroding and peeling. DEs and porosity were calculated, and are presented in Table 5 along with coating thicknesses.

Some combinations (M/M, L/M, M/L and L/L) led to an erosion of the first deposited layer or an erosion of the composite substrate. This observation confirms that M and L powders have too much kinetic energy and are able to erode the fragile interphase previously formed by isolated impinged particles.

F/F, M/F and L/F combinations led to a convenient coating build up. SEM cross section observations (Figure 9) were carried out, which reveals classical cold spray coating morphologies except for F/F sample which presents a 50 µm thick layer at the interface PEEK/coating with cracks and defects, as it was already observed in Figure 6. This can be correlated with the 2.00 ± 0.77 % porosity and 173 ± 16 µm coating thickness for this sample (Table 5), compared to 0.88 ± 0.22 % / 119 ± 14 µm and 0.94 ± 0.18 % / 106 ± 8 µm for M/F and L/F respectively. The 50 µm non-dense layer spotted on F/F increases both porosity and thickness values compared to other samples.

DEs of the second layers were quite stable on all samples with values between 34.8% and 36.9% (Table 5), which means that the F second layer deposition mechanism is similar regardless of which type of powder was used for the first layer.

It was possible to build a coating with Medium and Large particles on a Fine first layer, since this underlayer is not composed of isolated particles and therefore is mechanically resistant enough to withstand M and L particles impacts. However, those coatings partially peel during the projection (Figure 8). On both SEM cross observations, a layer with many cracks and defects can be spotted at the polymer/coating interface (Figure 10). This can be related to the observed peeling of the coating and the porosity of 2.18% and 1.3% for F/M and F/L respectively (Table 5).

The porosity value for F/L appears a bit low considering the aspect of the interface visible on Figure 10. This is due to the thresholding technique regardless porosity at the interface between PEEK and copper. Since porosity and PEEK appear almost the same color on SEM pictures, this porosity is often considered as PEEK by the software and therefore excluded from calculation. By manually modifying pictures in order to include those pores, the porosity value increases to 2.94% for F/L.

All samples which exhibit not continuous polymer/coating interface have been excluded from the next optimization step due to their porosity values, the thickest and densest coatings are recommended. Therefore, only M/F and L/F samples were selected for further experiments.

3.2.2   The Third Layer: Coatings Obtained With Alternating Powders

It was decided to add a third layer to increase the coating thickness. Samples M/F and L/F exhibited coating without interfacial defects but some porosities could still be spotted. Adding a layer of Fine powder would probably have increased the thickness, but as previously stated the hammering effect of this powder is low and therefore the porosity values were expected to be relatively high. The choice was made to spray M or L powder as a third layer, following an 'alternating powders' spray strategy which led to samples M/F/M and L/F/L (Figure 11). The spray process was successful, no delamination or peeling of the coatings were observed.

A thickness of 149 ± 8 µm (Table 6) was obtained for M/F/M, with a good interfacial PEEK/copper layer without visible cracks or porosity (Figure 12). The same morphology was observed for L/F/L but with a lower thickness (118 ± 20 µm).

The porosity was found to be the lowest of all the samples presented in this study, with respectively 0.35 ± 0.09 % and 0.50 ± 0.12 % for M/F/M and L/F/L (Table 6). Porosity

calculated in the middle of M/F/M thickness, corresponding roughly to the F layer, reached a value of only 0.12 ± 0.08 % which confirms an efficient compaction due to hammering effect induced by relatively large particles.

A DE increase from 5–8% to 12–13% can be observed for the third layer compared to the first one for both Medium and Large powders (Table 6). This probably indicates that the deposition mechanism switches from a 'metal on polymer' to a 'metal on metal' behavior. The DE value is still low for LPCS standards, usually around 30–40% for copper powders (as obtained for F powder in this study). This could be explained by the gas pressure and temperature used for spraying (8 bars, 330 °C, Table 2) which are below usual parameters used for spraying copper powder with such granulometry on metallic substrates. The stand-off distance set at 30 mm is also not standard, usually a 10 mm value is required for LPCS spraying, which could result in a lower DE.

M/F/M and L/F/L coatings were chemically etched to study the particles deformation and try to characterize the layers inside the coatings. An automatic threshold technique (GIMP software) was applied on SEM cross section observations. The software enhances first the contrast of pictures and then apply a binarization. This picture post-treatment reveals the shape of particles in the different layers, the particles being in white while the chemically etched joints between particles appear black. Two representative pictures are presented in Figure 13.

Starting from the bottom of the coatings, some relatively big particles can be spotted at the interface PEEK/coating, corresponding to the isolated impinged particles of the first M or L layer. The second layer coating of Fine particles can then be spotted. This layer densifies the first former by including small particles in the gaps between larger particles and then increases the coating thickness. A significant plastic deformation of Fine particles can be noticed.

The third layer composed of M or L can be discerned at the top, with particles diameters exceeding 20 µm on both coatings. Those particles present an important plastic deformation, which shows that underlying layers are dense and mechanically resistant enough to larger particle impacts.

The thickness of M/F and L/F layers was evaluated at 77 µm and 53 µm respectively (Figure 13). Those values are way lower than the measurements done on 2 layers coatings (119 ± 14

µm and 106 ± 8 µm, Table 5), with a decrease of 42 µm for M/F and 53 µm for L/F. This drop is directly induced by the addition of the third layer. This could be attributed to compaction by hammering effect since the final porosity in M/F/M and L/F/L was under 0.5 % (Table 6). Another explanation could be that using M and L powder for the third layer also erodes the previously deposited layers due to their high kinetic energy (Medium particles 10 times higher than Fine particles, Large particles 100 times, Table 4). The erosion leads to a loss of mass and therefore can be linked to the relatively low calculated DEs for the third layer (12–13 %).

3.3 Electrical resistivity

The main application of copper coatings on PEEK based composite is to enhance electrical properties for aerospace applications. Electrical resistivity of a metallic coating depends on several characteristics, such as their microstructure and presence of defects. Regarding Cold Spray coatings, two main factors can increase the resistivity such as the porosity and the presence of oxides [34], [35]. In this study, the porosity was minimized through the spraying strategy, to achieve a value of 0.35 ± 0.09 % for M/F/M sample (Table 6).

Four M/F/M samples were produced and their electrical resistivity was measured (Table 7). One Single PEEK sample without any copper coating was also tested to check the resistivity of the uncoated composite.

The modified composite is clearly electrically resistant, with a resistivity of $1.4.10^8 \pm 1.10^6$ Ω.cm. The addition of a copper coating induces a drop of the resistivity to $5\text{–}6.10^{-3} \pm 1.2.10^{-3}$ Ω.cm which corresponds to the resistivity variation between samples due to coating thickness modification.

Regarding LPCS coatings, Małachowska and al. [35] obtained a value of 26.10^{-6} Ω.cm by spraying copper on a PVC substrate with a $Sn + Al_2O_3$ intermediate layer. Koivuluoto and al. [36] compared LPCS and HPCS (High Pressure Cold Spray) copper coatings on grit-blasted carbon steel. Values for LPCS in this study were at $3.7.10^{-6}$ Ω.cm for pure Cu coating and

$2.8.10^{-6}$ Ω.cm for Cu + Al_2O_3 coating. They obtained a resistivity of $2.2.10^{-6}$ Ω.cm for HPCS pure Cu coatings, really close to the value of bulk Cu at ambient temperature ($1.7.10^{-6}$ Ω.cm [37]). Another HPCS studies reported values of 10^{-5}–10^{-6} Ω.cm [34], [38]. Ohmann [39] measured resistivity of exceeding 10^5 Ω.cm for a copper coating containing 0.21% oxygen, but exhibiting high porosity and bad particle deformations.

The resistivity values obtained on M/F/M samples are 1000 times higher than the best ones reported in other studies. Since porosity was measured at 0.35 ± 0.09 %, this parameter is not considered as responsible for the high resistivity. Oxides in the powders can be mostly considered. Indeed, the use of low gas temperature and pressure on composite do not break the oxide layer on particles upon impact. A poor bonded region between particles occurred leading to oxidation.

3.4 Influence of the PEEK film thickness on the spraying strategy

After developing the spray strategy on Single PEEK (57 µm) samples, the effect of the PEEK film thickness was investigated by carrying out exactly the same spray strategy on Double PEEK (105 µm) samples.

The obtained results were similar for almost all Single and Double PEEK samples, regarding deposition behavior, coating morphologies, thicknesses, DEs and porosity values. The only differences were for the two-layer coatings elaborated using F/M and F/L powder combinations. As already shown in Figure 8, Single PEEK samples with F/M and F/L present a peeling behavior. When spraying the same powder combinations on Double PEEK samples a coating was obtained for both cases, without any peeling (Figure 14).

SEM cross-section observations (Figure 15) of both Single and Double PEEK samples revealed a possible explanation of this difference.

While Single PEEK samples exhibit coating/polymer interface without well compacted and homogeneous layer (Figure 9 and Figure 10), Double PEEK samples present a thinner interface reducing cracks and defects (Figure 15).

Such irregular interface on Single PEEK samples can be responsible for the observed peeling when this base is hammered by incoming particles, while spraying the second layer.

When the PEEK film is thicker, a greater contribution of the elastic modulus and elasto-plastic behavior of the PEEK can be assumed. This leads to a reduced rebound phenomenon

for the incoming particles and therefore a more compact interface for Double PEEK samples. This layer appears to be sufficiently resistant to withstand the impact of incoming particles regardless of the powder, which explains why the coating is growing instead of peeling for those samples.

4 Conclusion

A new way to produce copper coatings on CFRP with Low Pressure Cold Spray was investigated. Using powders with defined granulometry, coatings have then been optimized.

Although thick coatings (300 µm) were first obtained by using only Fine powder, the best results were obtained via alternating powders to reach thick coatings.

First, Medium or Large powder were used as the first layer to insert large copper particles on the substrate surface. Then, in a second time, Fine powder was sprayed to densify this layer by inserting small particles in the gaps between previously deposited larger particles. The coating was then mechanically resistant enough to the impacts of Medium or Large particles sprayed on top. Impact behavior switched from a 'metal on polymer' to 'metal on metal'.

This third layer densified the subsequent layers by hammering effect and porosities of the coatings were calculated at $0.35 \pm 0.09\%$ for M/F/M and $0.50 \pm 0.12\%$ for L/F/L, for respective thicknesses of 149 ± 8 µm and 118 ± 20 µm.

A PEEK film thickness of approximately 50 µm was in good accordance with elaboration of coatings and the need for matrix layer on the surface of the composite was shown. It was demonstrated that PEEK film thickness influenced only coatings built with Fine powder as the first layer.

Additional work is still needed to qualify and quantify the influence of the PEEK layer thickness, numerical and experimental considerations are under investigation. In this study spray parameters were fixed. A parameter optimization process could then be carried out to improve deposition efficiencies. Then, mechanical characterizations of the coatings such as adhesion tests have to be carried out.

Electrical resistivity of M/F/M coatings, considered as the best ones obtained in this study, was tested and measured at $5\text{--}6.10^{-3} \pm 1.2.10^{-3}$ Ω.cm. This value was compared to literature and found to be 1000 times higher than the best values but also way lower than the worst ones (10^{5} Ω.cm). The high resistivity is a consequence of the oxygen content in the powders and

the low gas pressure and temperature used to spray on composite. More studies are needed to confirm this hypothesis regarding the influence of oxygen content on resistivity values.

Acknowledgments

References

[1]   C. Soutis, "Carbon fiber reinforced plastics in aircraft construction," *Mater. Sci. Eng. A*, vol. 412, no. 1–2, pp. 171–176, 2005.

[2]   J. Villoutreix and J. Acetarin, "Polyétheréthercétone Polyétheréthercétone (PEEK)," vol. 33, no. 0, 2017.

[3]   S. Najeeb, M. S. Zafar, Z. Khurshid, and F. Siddiqui, "Applications of polyetheretherketone (PEEK) in oral implantology and prosthodontics," *J. Prosthodont. Res.*, vol. 60, no. 1, pp. 12–19, 2016.

[4]   P. Cebe, S. Chung, and S. Hong, "Effect of Thermal History on Mechanical Properties of polyetheretherketone Below the Glass Transition Temperature," *J. Appl. Polym. Sci.*, vol. 33, pp. 487–503, 1987.

[5]   J. Denault, C. Canada, M. Dumouchel, and A. Division, "Consolidation Process of PEEK / Carbon Composite for Aerospace Applications," *Adv. Perform. Mater.*, vol. 5, pp. 83–96, 1998.

[6]   A. Larsson, "The interaction between a lightning flash and an aircraft in flight," *Appl. Phys.*, vol. 3, pp. 1423–1444, 2002.

[7]   M. Gagné and D. Therriault, "Lightning strike protection of composites," *Prog. Aerosp. Sci.*, vol. 64, pp. 1–16, 2014.

[8]   H. Kawakami and P. Feraboli, "Lightning strike damage resistance and tolerance of scarf-repaired mesh-protected carbon fiber composites," *Compos. Part A*, vol. 42, no. 9, pp. 1247–1262, 2011.

[9]   "http://www.astrosealproducts.com/index.html." .

[10] F. Decla, "Metalisation of an organic matric composite (CFRP) with Plasma Spray," Ecole nationale suprieure des mines de Paris, FRANCE, 1997.

[11] S. Vyawahare, "Protective thermal spray coatings for polymer matrix composites," Faculty of the Graduate School of Wichita State University, 2006.

[12] J. K. Sutter and R. Cupp, "Erosion Coatings for Polymer Matrix Composites in Propulsion Applications," pp. 421–440, 2003.

[13] R. Gonzalez, H. Ashrafizadeh, A. Lopera, P. Mertiny, and A. Mcdonald, "A Review of Thermal Spray Metallization of Polymer-Based Structures," *J. Therm. Spray Technol.*, vol. 25, no. 5, pp. 897–919, 2016.

[14] R. Lupoi and W. O'Neill, "Deposition of metallic coatings on polymer surfaces using cold spray," *Surf. Coatings Technol.*, vol. 205, no. 7, pp. 2167–2173, 2010.

[15] Z. D. Cheng, M. Y. Cao, and B. Wunderlich, "Glass Transition and Melting Behavior of Poly (oxy- 1,4-phenyleneoxy- 1,4-phenylenecarbonyl- 1,4-phenylene)," *Macromolecules*, pp. 1868–1876, 1986.

[16] R. Li, "Time-temperature superposition method for glass transition temperature of plastic materials," *Mater. Sci. Eng. A*, vol. 278, no. 1–2, pp. 36–45, 2000.

[17] D. Giraud, "Study of the mechanical and metallurgical contributions ot coating-substrate bonding in cold spray for 'Aluminum/Polyamide 66' and 'Titanium/Ti-6Al-4V,'" Ecole Nationale Supérieure des Mines de Paris, 2014.

[18] X. L. Zhou, a. F. Chen, J. C. Liu, X. K. Wu, and J. S. Zhang, "Preparation of metallic coatings on polymer matrix composites by cold spray," *Surf. Coatings Technol.*, vol. 206, no. 1, pp. 132–136, 2011.

[19] J. Affi, H. Okazaki, M. Yamada, and M. Fukumoto, "Fabrication of Aluminum Coating onto CFRP Substrate by Cold Spray," *Mater. Trans.*, vol. 52, no. 9, pp. 1759–1763, 2011.

[20] H. Q. Che and S. Yue, "Cold Spray of Carbon Fiber Reinforced Polymer for Lightning Strike Protection," in *Proceedings of the International Thermal Spray Conference*, 2014, pp. 497–499.

[21] H. Q. Che, S. Yue, and P. Vo, "Cold Spray onto Carbon Fiber Reinforced Polymers for lightning strike protection," in *Proceedings of the International Thermal Spray Conference*, 2016.

[22] R. R. Rogers and J. F. Fydell, "Factors Affecting the Transformation of Gray Tin at Low Temperatures," *J. Electrochem. Soc.*, vol. 100, pp. 383–387, 1953.

[23] G. Archambault, B. Jodoin, S. Gaydos, and M. Yandouzi, "Metallization of carbon

fiber reinforced polymer composite by cold spray and lay-up molding processes," *Surf. Coatings Technol.*, vol. 300, pp. 78–86, 2016.

[24] H. Che, X. Chu, P. Vo, and S. Yue, "Metallization of Various Polymers by Cold Spray," *J. Therm. Spray Technol.*, vol. 27, no. 1, pp. 169–178, 2018.

[25] "http://www.porcher-ind.com/uploads/files/Selector_Guide_Pipreg2014.pdf." .

[26] "http://www.lipp-terler.com/index.php?page=03english-lite-tk-mod." .

[27] J. Laplume, "Bases théoriques de la mesure de la résistivité et de la constant de Hall par la méthode des pointes." 1955.

[28] F. Smits, "Measurement of sheet resistivities with the four-point probe," *Bell System Technical Journal*, vol. 34. pp. 711–718, 1958.

[29] I. Burlacov, J. Jirkovský, L. Kavan, R. Ballhorn, and R. B. Heimann, "Cold gas dynamic spraying (CGDS) of TiO2 (anatase) powders onto poly(sulfone) substrates: Microstructural characterisation and photocatalytic efficiency," *J. Photochem. Photobiol. A Chem.*, vol. 187, no. 2–3, pp. 285–292, 2007.

[30] H. Koivuluoto and P. Vuoristo, "Effect of Powder Type and Composition on Structure and Mechanical Properties of Cu + Al2O3 Coatings Prepared by using Low-Pressure Cold Spray Process," *J. Therm. Spray Technol.*, vol. 19, no. 5, pp. 1081–1092, 2010.

[31] S. V. Klinkov, V. F. Kosarev, and M. Rein, "Cold spray deposition: Significance of particle impact phenomena," *Aerosp. Sci. Technol.*, vol. 9, no. 7, pp. 582–591, 2005.

[32] E. Irissou, J. G. Legoux, B. Arsenault, and C. Moreau, "Investigation of Al-Al 2O 3 cold spray coating formation and properties," *J. Therm. Spray Technol.*, vol. 16, no. 5–6, pp. 661–668, 2007.

[33] T. Schmidt, F. Gärtner, H. Assadi, and H. Kreye, "Development of a generalized parameter window for cold spray deposition," *Acta Mater.*, vol. 54, no. 3, pp. 729–742, 2006.

[34] R. C. McCune, W. T. Donlon, O. O. Popoola, and E. L. Cartwright, "Characterization of Copper Layers Produced by Cold Gas-Dynamic Spraying," *J. Therm. Spray Technol.*, vol. 9, no. 1, pp. 73–82, 2000.

[35] A. Ma *et al.*, "Possibility of spraying of copper coatings on polyamide 6 with low pressure cold spray method," *Surf. Coat. Technol.*, pp. 1–8, 2017.

[36] H. Koivuluoto, A. Coleman, K. Murray, M. Kearns, and P. Vuoristo, "High Pressure Cold Sprayed (HPCS) and Low Pressure Cold Sprayed (LPCS) Coatings Prepared from OFHC Cu Feedstock : Overview from Powder Characteristics to Coating Properties," vol. 21, no. September, pp. 1065–1075, 2012.

[37] R. A. Matula, "Electrical Resistivity of Copper, Gold, Palladium and Silver," *J. Phys. Chem. Ref. Data*, pp. 1147–1297, 1979.

[38] A. Ganesan, J. Af, M. Yamada, and M. Fukumoto, "Bonding behavior studies of cold sprayed copper coating on the PVC polymer substrate," *Surf. Coat. Technol.*, vol. 207, pp. 262–269, 2012.

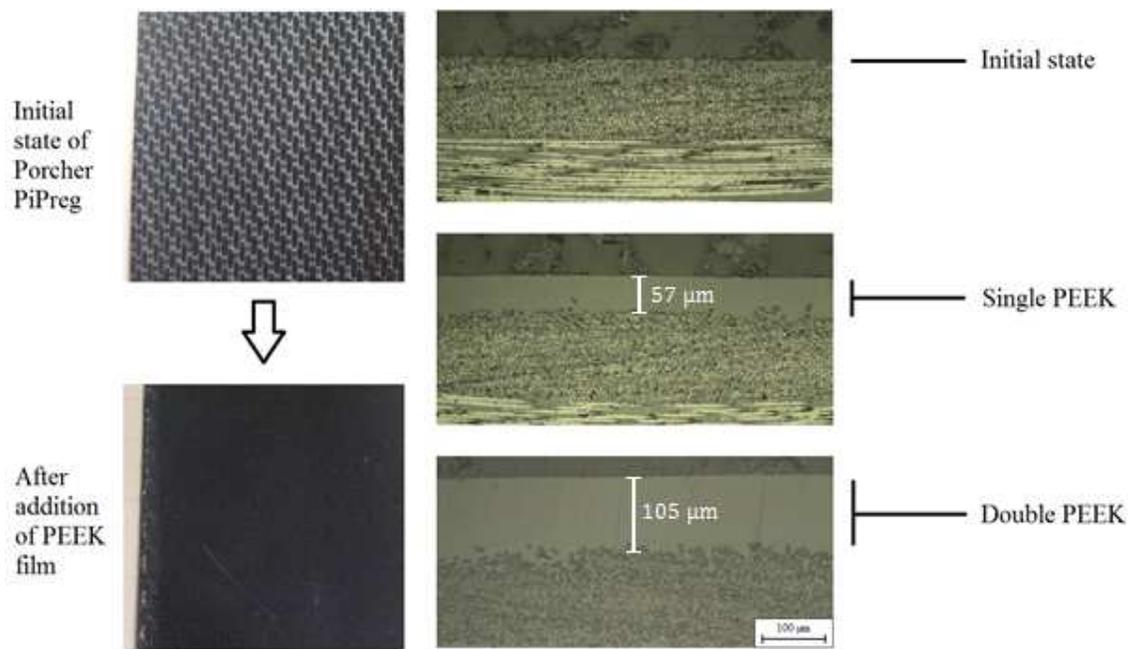[39] D. Ohmann, "Master's Thesis, University of Wisconsin, Madison," 1998.

Figure captions

Figure 1: a) Surface views before and after addition of PEEK film, b) Cross-section observations by optical microscopy of raw, Single PEEK and Double PEEK samples (100X)
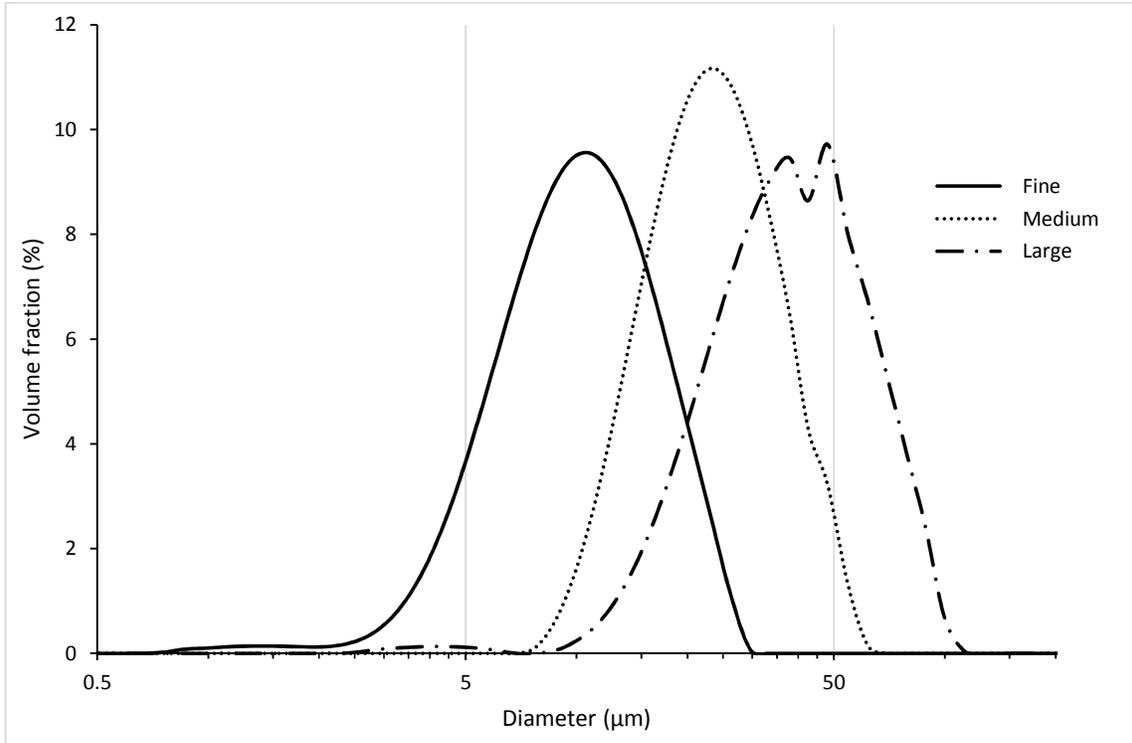
Figure 2: Particles diameter distribution of powders
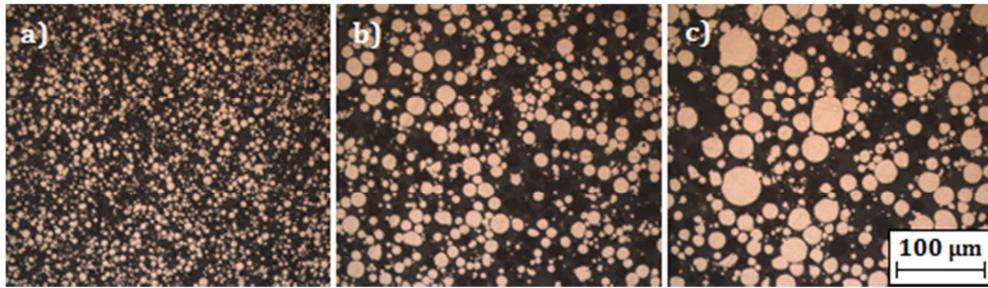
Figure 3: Observation by optical microscopy of Fine (a), Medium (b) and Large (c) powders (100X)
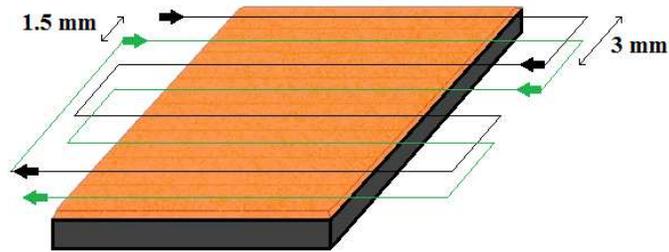
Figure 4: Scheme of the robot scan movements to spray a complete layer of copper on composites, a coating being composed of one or several layers on top of each others
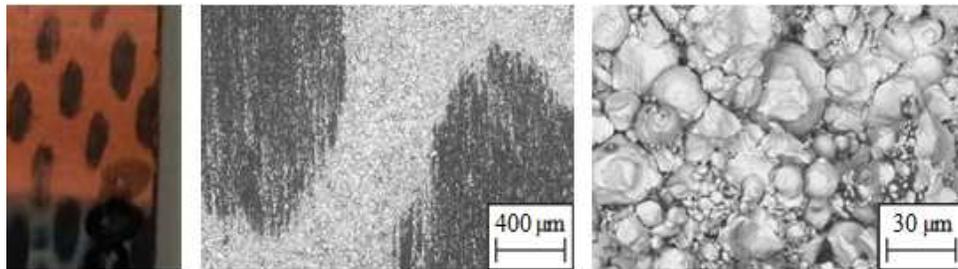
Figure 5: Macro-morphology and SEM observation of a non-modified sample after spraying (80X and 1000X)
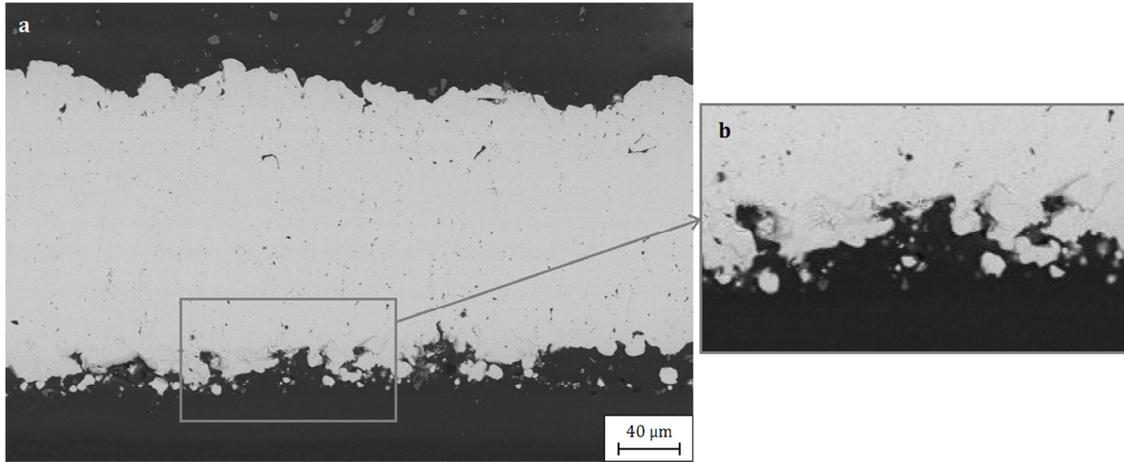
Figure 6: (a) SEM cross section observation (500X). (b) Zoom on the interface with some visible cracks and defects
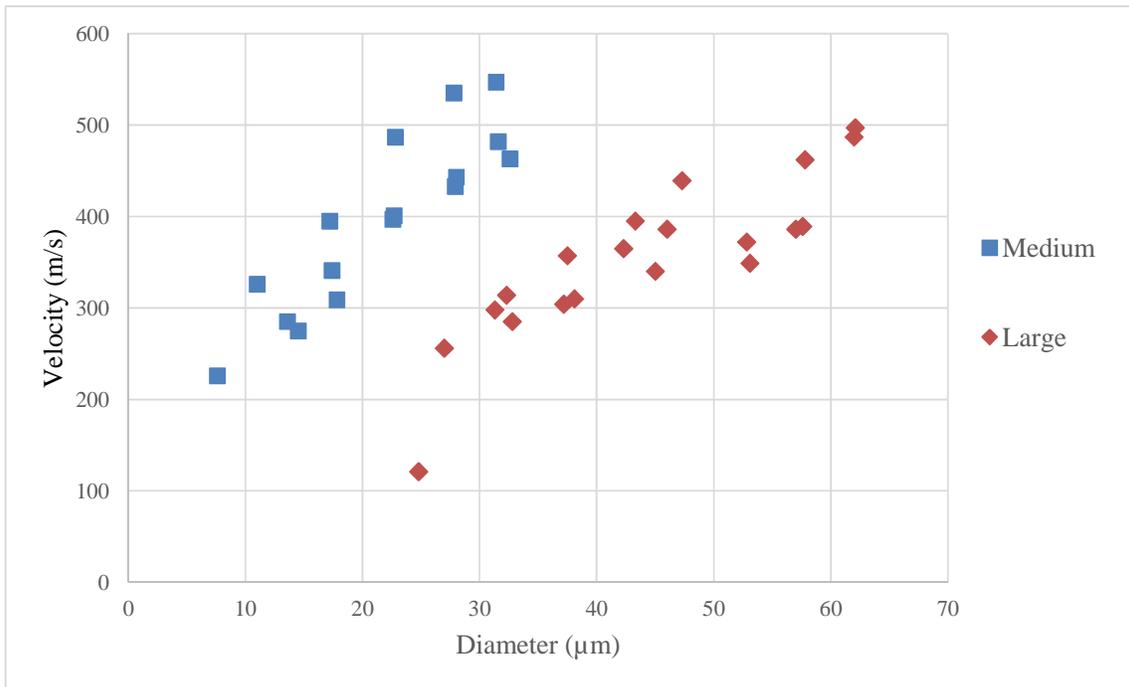
Figure 7: In-flight particles velocities for Medium and Large powders (DPV measurement)
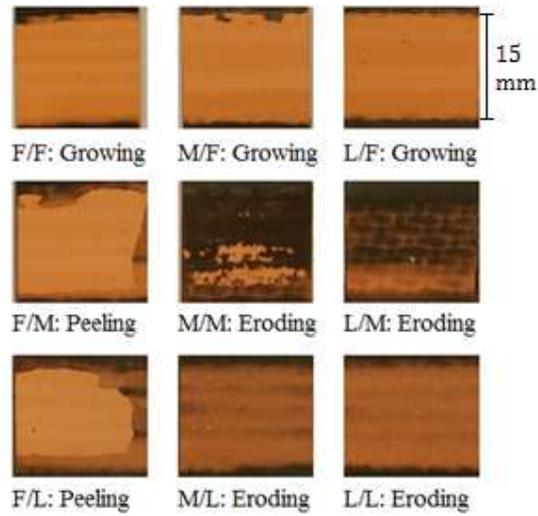
Figure 8: Macro-morphology of samples with 2 coating layers

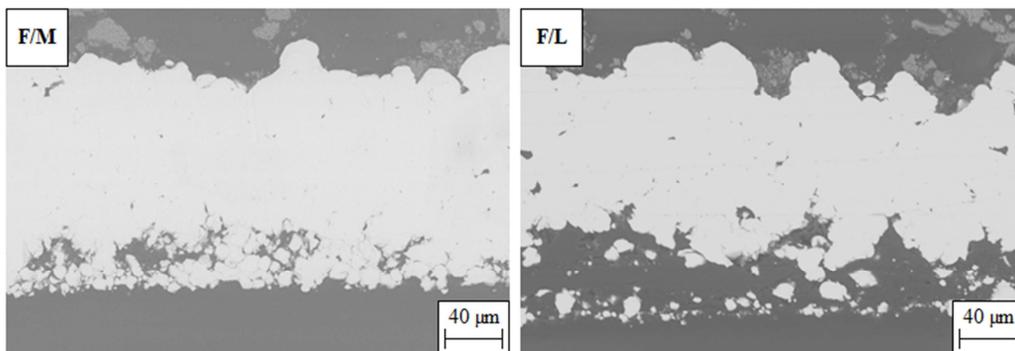Figure 9: SEM cross section observations of F/F, M/F and L/F samples (800X)

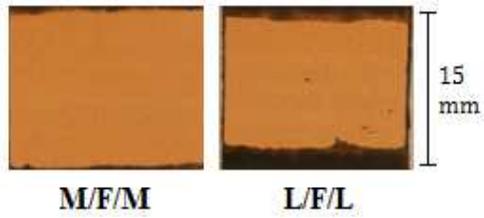Figure 10: SEM cross section observations of F/M and F/L samples (800X)

Figure 11: Macro-morphology of coatings produced with alternating powders spraying strategy
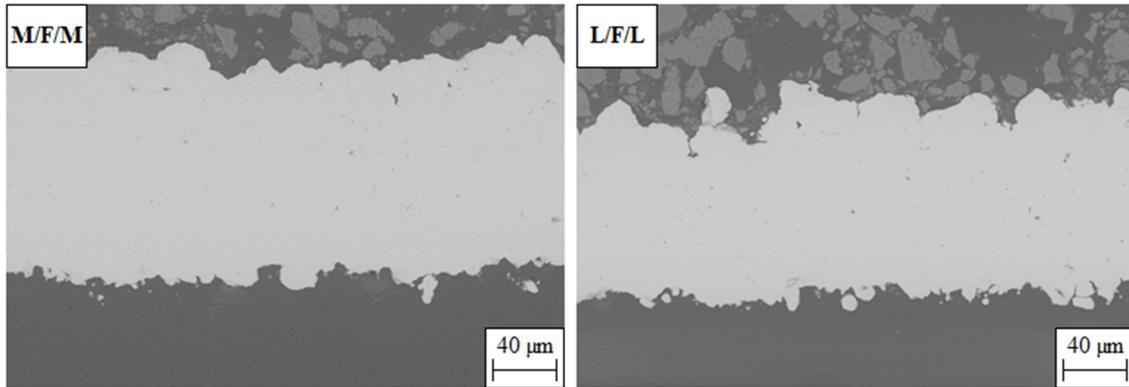

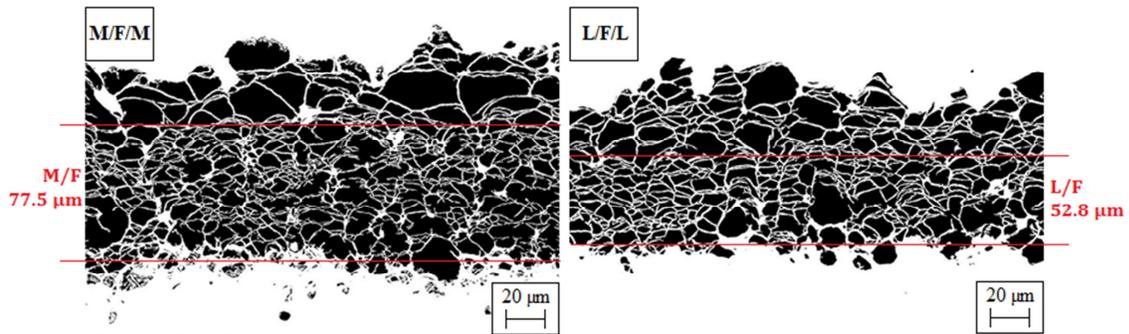Figure 12: SEM cross section observations of M/F/M and L/F/L samples (800X)

Figure 13: Post-treated pictures of M/F/M and L/F/L chemically etched samples
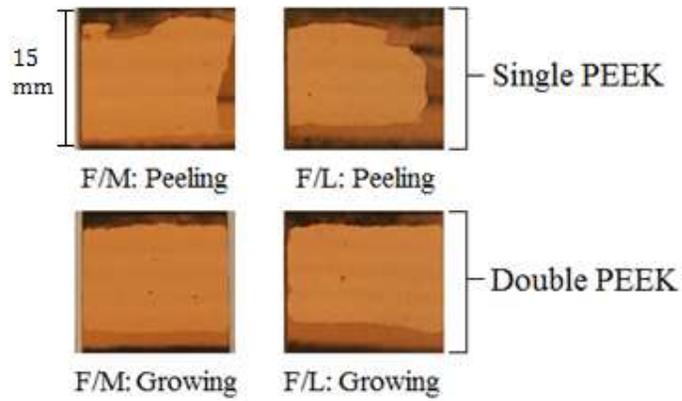
Figure 14: Macro-morphology of Single and Double PEEK 2-layers samples, with Fine powder as first layer
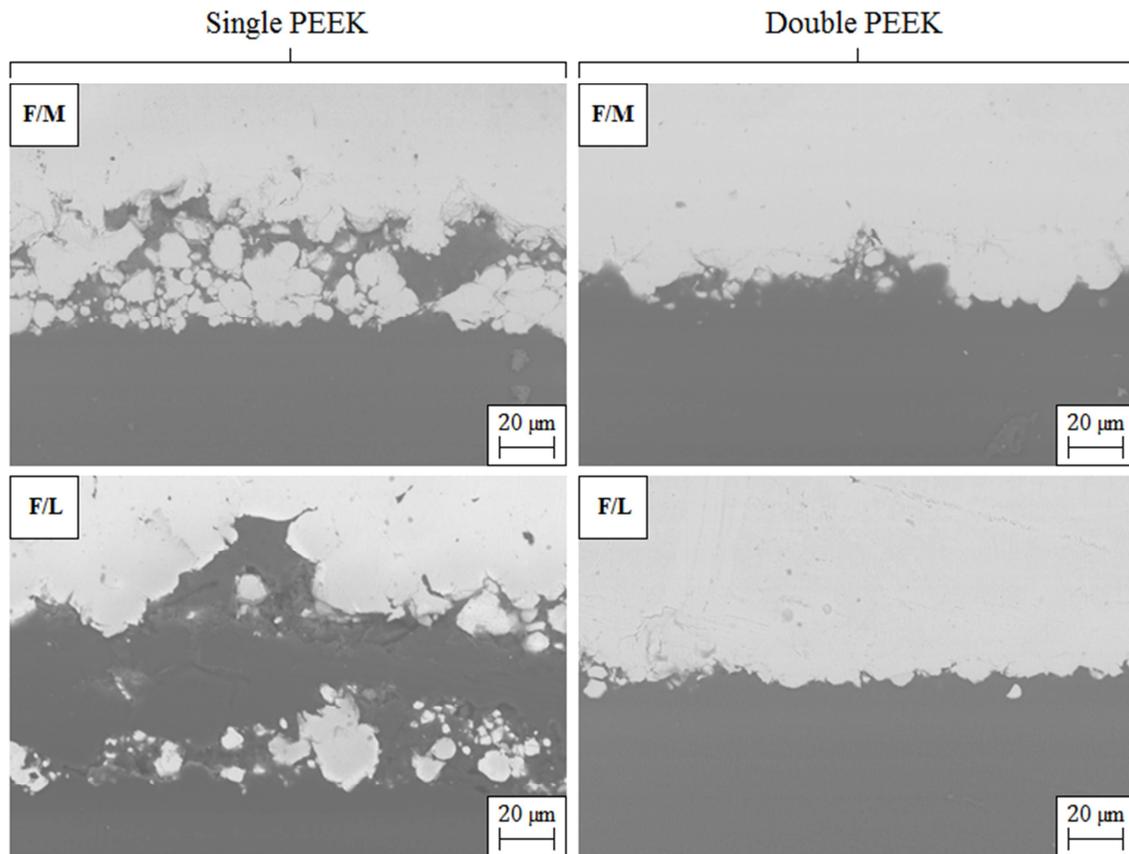

Figure 15: SEM cross section observations of PEEK-coating interfaces of F/F, F/M and F/L for Single and Double samples (1500x)

Tables

Table 1: Volume deciles of the three Cu – 0.1% Ag powders

Powder	d_{10} (µm)	d_{50} (µm)	d_{90} (µm)
Fine (F)	5.1	10.1	18.3
Medium (M)	13.6	23.2	39.4
Large (L)	19.3	37.9	68.6

Table 2: Spray parameters used for LPCS process implementing Cu-Ag powders

CARRIER GAS	N_2
INLET GAS PRESSURE [bars]	8
NOZZLE OUTLET GAS TEMPERATURE [°C]	330
STAND-OFF DISTANCE [mm]	30
SCAN SPEED [mm/s]	100
COOLING TIME [s]	3

Table 3: Surface morphology, DEs and cross section observations of first deposited layers according to the powder granulometry

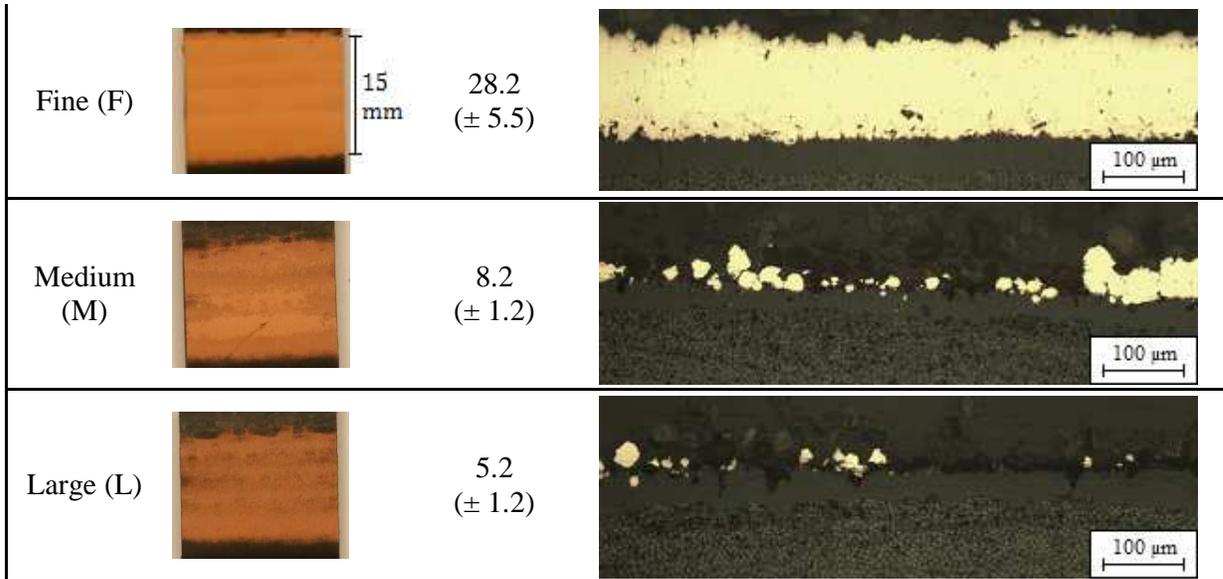| Powder	Surface picture	DE (%)	Cross Sections (optical microscopy, 100X)

Fine (F)	15 mm	28.2 (± 5.5)	100 µm
Medium (M)		8.2 (± 1.2)	100 µm
Large (L)		5.2 (± 1.2)	100 µm

Table 4: Evaluation of kinetic energy for each powder median diameter

Powder	d_{50} (µm)	Mass (kg)	E_c (kg.m^2.s^{-2})
Fine (F)	10.1	$4.8.10^{-12}$	$3.9.10^{-7}$
Medium (M)	23.2	$5.9.10^{-11}$	$4.7.10^{-6}$
Large (L)	37.9	$2.6.10^{-10}$	$2.0.10^{-5}$

Table 5: DEs, thickness and porosity of 2-layer coatings

	1st layer DE (%)	2nd layer DE (%)	Thickness (µm)	Porosity (%)
F/F	27.8	36.7	173 ± 16	2.00 ± 0.77
M/F	8.6	34.8	119 ± 14	0.88 ± 0.22
L/F	6.9	36.9	106 ± 8	0.94 ± 0.18
F/M	24.2	15.4	164 ± 9	2.18 ± 0.45
F/L	28.7	15.4	135 ± 11	1.30 ± 0.41

Table 6: DEs and thickness of 3 layers coatings. DE of the second layer for L/F/L is missing due to a measurement error of the deposited mass.

	Single PEEK				
	1st layer DE (%)	2nd layer DE (%)	3rd layer DE (%)	Thickness (µm)	Porosity (%)
M/F/M	7.9	31.9	11.8	149 ± 8	0.35 ± 0.09
L/F/L	5.3	/	13.0	118 ± 20	0.50 ± 0.12

Table 7: Electrical resistivity measurements

Sample	Composite	MFM1	MFM2	MFM3	MFM4
Coating thickness (µm)	/	126 ± 12	138 ± 10	164 ± 17	159 ± 11
Electrical resistivity (Ω.cm)	$1.4.10^{8}$ $\pm 1.0.10^{6}$	$5.1.10^{-3}$ $\pm 1.2.10^{-3}$	$5.1.10^{-3}$ $\pm 1.3.10^{-3}$	$6.5.10^{-3}$ $\pm 1.6.10^{-3}$	$6.2.10^{-3}$ $\pm 1.2.10^{-3}$